



Hu, H., Liu, X.-J., & Modugno, M. (2003). Expansion of a quantum degenerate boson-fermion mixture.

Originally published in *Physical Review A: Atomic, Molecular, and Optical Physics*, 67(6).
Available from: <http://dx.doi.org/10.1103/PhysRevA.67.063614>.

Copyright © 2003 The American Physical Society.

This is the author's version of the work. It is posted here with the permission of the publisher for your personal use. No further distribution is permitted. If your library has a subscription to this journal, you may also be able to access the published version via the library catalogue.

The definitive version is available at <http://pra.aps.org/>.



Expansion of a quantum degenerate boson-fermion mixture

Hui Hu¹, Xia-Ji Liu^{2,3} and Michele Modugno⁴

¹*Abdus Salam International Center for Theoretical Physics, P. O. Box 586, Trieste 34100, Italy*

²*LENS, Università di Firenze, Via Nello Carrara 1, 50019 Sesto Fiorentino, Italy*

³*Institute of Theoretical Physics, Academia Sinica, Beijing 100080, China*

⁴*INFN, LENS and Dipartimento di Fisica, Università di Firenze,
Via Nello Carrara 1, 50019 Sesto Fiorentino, Italy*

(February 2, 2008)

We study the expansion of an ultracold boson-fermion mixture released from an elongated magnetic trap, in the context of a recent experiment at LENS (G. Roati *et al.*, Phys. Rev. Lett. **89**, 150403 (2002)). We discuss in some details the role of the boson-fermion interaction on the evolution of the radial-to-axial aspect ratio of the condensate, and show that it depends crucially on the relative dynamics of the condensate and degenerate Fermi gas in the radial direction, which is characterized by the ratio between the trapping frequency for fermions and for bosons. Our numerical simulations are in reasonable agreement with the experiment.

PACS numbers:03.75.Fi, 05.30.Fk, 05.30.Jp, 67.60.-g

I. INTRODUCTION

The experimental realization of ultracold bose-fermi mixtures of alkali atoms introduces a novel tool for the study of various quantum phenomena [1–4]. The most appealing one is certainly the Bardeen-Cooper-Schrieffer (BCS) type superfluidity, since the presence of boson-fermion interaction in the mixture is expected to induce an effective attraction between fermions by exchanging density fluctuations of the bosonic background [5,6], analogously to that of superfluid ³He and ⁴He in low-temperature physics [7,8]. With this respect, the recently reported quantum degenerate mixtures of ⁴⁰K (fermion) and ⁸⁷Rb (boson) by the LENS group would be particularly interesting due to the *large* boson-fermion attraction, which has been directly manifested by the collapse of the degenerate fermions above a critical number of particles [4], or alternatively, by the observation that the Bose-Einstein condensate (BEC) coexisting with the Fermi gas inverts its aspect ratio more rapidly than a pure condensate during the ballistic expansion [3]. In the latter case, the experimental result agrees qualitatively with the expectations of a tighter confinement for a BEC in a Fermi gas with mutual attraction [9,10], and is qualitatively fitted by the theoretical predictions for the free expansion of a pure BEC with trap frequencies 10% larger than the actual one. However, possible effects of the boson-fermion attraction *during* the early stages of the expansion are not considered in the fitting and certainly need a further investigation.

In this paper, we would like to study in details the effect of the boson-fermion attraction on the expansion of the condensate as well as of the Fermi gas after the release from the strongly elongated magnetic trap. We have taken into account both ground state effects and the effect of attraction between bosons and fermions during the early stages of the expansion. The latter one is found to play an important role on the evolution of the radial-to-axial aspect ratio of the condensate. Our numerical

simulations are in reasonable agreement with the experiment.

II. FORMULATION

We consider a dilute spin-polarized boson-fermion binary mixture at very low temperature trapped in a strongly elongated harmonic oscillator potential. In the semi-classical Thomas-Fermi approximation, the condensate and degenerate Fermi gas evolve according to the Stringari's hydrodynamic formulation [11]

$$\begin{aligned} \frac{\partial n_b}{\partial t} + \nabla \cdot (n_b \mathbf{v}_b) &= -\Gamma_{coll}, \\ m_b \frac{\partial \mathbf{v}_b}{\partial t} + \nabla \cdot \left(V_{ho}^b + g_{bb} n_b + g_{bf} n_f + \frac{1}{2} m_b \mathbf{v}_b^2 \right) &= 0, \end{aligned} \quad (1)$$

and Boltzmann-Vlasov kinetic equation [12,13],

$$\frac{\partial f}{\partial t} + \mathbf{v}_f \cdot \frac{\partial f}{\partial \mathbf{r}} - \frac{1}{m_f} \frac{\partial V_{ho}^f}{\partial \mathbf{r}} \cdot \frac{\partial f}{\partial \mathbf{v}_f} - \frac{g_{bf}}{m_f} \frac{\partial n_b}{\partial \mathbf{r}} \cdot \frac{\partial f}{\partial \mathbf{v}_f} = I_{coll}, \quad (2)$$

respectively. Here $f(\mathbf{r}, \mathbf{v}_f, t)$ is the single particle phase space distribution function for fermions; $n_b(\mathbf{r}, t)$, $n_f(\mathbf{r}, t) = \int d^3 \mathbf{v}_f f(\mathbf{r}, \mathbf{v}_f, t)$ and $\mathbf{v}_b(\mathbf{r}, t)$, $\mathbf{v}_f(\mathbf{r}, t)$ are the densities and velocity fields for bosons and fermions, respectively. Here, for simplicity, we consider the case in which they are trapped by symmetric confining potentials, $V_{ho}^{b,f}(\mathbf{r}) = \frac{1}{2} m_{b,f} (\omega_{\perp,b,f}^2 \rho^2 + \omega_{z,b,f}^2 z^2)$, in a *concentric* configuration. Note that in the realistic experimental situation the centers of mass of the condensate and Fermi gas are instead *displaced* due to the different gravitational sag for ⁴⁰K and ⁸⁷Rb [3]. The displacement is not sufficiently large to affect the geometrical overlap of the two degenerate species. However, in some degree it reduces the boson-fermion attraction. Of course, a quantitative

analysis should take into account this displacement. We will comment on this point later.

The influence of the interatomic scattering processes between the two species on their dynamics has been taken into account in two parts: mean fields and collisions. In the above equations, the term $g_{bf}n_b(\mathbf{r}, t)$ and $g_{bf}n_b(\mathbf{r}, t)$ are included as the Hartree-Fock mean field effect of boson-fermion interaction [14] (note that the latter one is known as the Vlasov contribution in the literatures). The boson-boson and boson-fermion interaction strength for the pseudopotentials, g_{bb} and g_{bf} , are related to the s -wave scattering lengths a_{bb} and a_{bf} through $g_{bb} = 4\pi\hbar^2 a_{bb}/m_b$, $g_{bf} = 2\pi\hbar^2 a_{bf}/m_{bf}$, in which $m_{bf} = m_b m_f / (m_b + m_f)$ is the reduced boson-fermion mass. On the other hand, the dissipation term $-\Gamma_{coll}$ or I_{coll} accounts for collisions [15]. The relative importance of the mean field and dissipation terms in describing the dynamics of whole system depends upon the rate of collisions compared to the characteristic time scale of the single particle oscillation. When collisions are relatively rare, the mean-field interaction dominates and the system is in the collisionless regime. In the opposite, hydrodynamic regime, the degenerate Fermi gas is always in the local equilibrium with the condensate [16]. The dynamics is then most appropriately described by the hydrodynamic Euler equation of motion [17,18]. Due to the lack of information on the collision rate in experiment, we shall mainly focus on the collisionless regime by neglecting the dissipation terms $-\Gamma_{coll}$ and I_{coll} . The opposite hydrodynamic regime will be briefly discussed at the end of this paper.

In the absence of the boson-fermion interaction ($g_{bf} = 0$) and dissipation terms, both the Eqs. (1) and (2) admit a simple scaling solution, *i.e.*,

$$\begin{aligned} n_b(\mathbf{r}, t) &= \frac{1}{\prod_j b_j(t)} n_b^0 \left(\frac{r_i}{b_i(t)} \right), \\ v_{b_i}(\mathbf{r}, t) &= \frac{1}{b_i(t)} \frac{db_i(t)}{dt} r_i, \end{aligned} \quad (3)$$

for the condensate [18,19] and

$$\begin{aligned} f(\mathbf{r}, \mathbf{v}_f, t) &= f_0 \left(\frac{r_i}{\gamma_i(t)}, \mathbf{V}(\mathbf{r}, t) \right), \\ V_i(\mathbf{r}, t) &= \gamma_i(t) v_{f_i} - \frac{d\gamma_i(t)}{dt} r_i, \end{aligned} \quad (4)$$

for the degenerate Fermi gas [12,13,20]. Here n_b^0 and f_0 are the equilibrium distributions. The dependence on time t is entirely contained the six dimensionless scaling parameters, $b_i(t)$ and $\gamma_i(t)$, where $i = x, y$, and z . By substituting this solution into Eqs. (1) and (2), it is easily to show that, the scaling parameters obey the differential equations [19,20],

$$\ddot{b}_i(t) + \omega_{ib}^2(t) b_i(t) - \frac{\omega_{ib}^2(0)}{b_i(t) \prod_j b_j(t)} = 0, \quad (5)$$

$$\ddot{\gamma}_i(t) + \omega_{if}^2(t) \gamma_i(t) - \frac{\omega_{if}^2(0)}{\gamma_i^3(t)} = 0. \quad (6)$$

Solutions of Eqs. (5) and (6), respectively, determine the time evolution of the pure condensate and Fermi gas. In particular, they can be used to study the expansion of the system after a sudden and total opening of the trap at $t = 0$. For an elongated cylindrical trap with anisotropic parameter $\lambda = \omega_{zb}/\omega_{\perp b} (= \omega_{zf}/\omega_{\perp f}) \ll 1$, one may find that [19,20]

$$\begin{aligned} b_{\perp}(\tau) &= \sqrt{1 + \tau^2}, \\ b_z(t) &= 1 + \lambda^2 \left[\tau \arctan \tau - \ln \sqrt{1 + \tau^2} \right], \end{aligned} \quad (7)$$

and

$$\begin{aligned} \gamma_{\perp}(\tau) &= \sqrt{1 + \beta^2 \tau^2}, \\ \gamma_z(\tau) &= \sqrt{1 + \lambda^2 \beta^2 \tau^2}, \end{aligned} \quad (8)$$

where we have introduced a dimensionless time variable $\tau = \omega_{\perp b} t$ and $\beta = \omega_{\perp f}/\omega_{\perp b}$.

In the presence of the boson-fermion interaction ($g_{bf} \neq 0$), however, the simple scaling solution is no longer satisfied at every position \mathbf{r} after the substitution. A useful approximation, in the first order of g_{bf} , is to assume the scaling form of the solution a priori, and fulfill it *on average* by integrating over the spatial coordinates. This strategy has been recently used by Guery-Odelin [12] to investigate the effect of the interaction on the collective oscillation of a classical gas in the collisionless regime and by Menotti *et al.* to study the expansion of an interacting Fermi gas [13]. In some sense, this approximation is equivalent to the sum-rule approach [13] that is extensively used in evaluating the low-energy collective modes of dilute quantum gases [11]. We have also recently applied this approximation to derive the coupled set of differential equations for $b_i(t)$ and $\gamma_i(t)$, and studied the monopole and quadrupole excitations of boson-fermi mixtures after linearizing these equations around the equilibrium points [21]. Here we only present the brief derivation to make the paper self-contained.

As specified above, we substitute the scaling ansatz Eq. (3) into Stringari's hydrodynamic equations. By setting $R_i = r_i/b_i(t)$, one finds,

$$\begin{aligned} \ddot{b}_i(t) R_i + \omega_{ib}^2(t) b_i(t) R_i + \frac{g_{bb}}{m_b} \frac{1}{b_i(t) \prod_j b_j(t)} \frac{\partial n_b^0(\mathbf{R})}{\partial R_i} \\ + \frac{g_{bf}}{m_b} \frac{1}{b_i(t) \prod_j \gamma_j(t)} \frac{\partial n_f^0 \left(\frac{b_i(t)}{\gamma_i(t)} R_i \right)}{\partial R_i} = 0. \end{aligned} \quad (9)$$

The coupled differential equations for the scaling parameters $b_i(t)$ can be obtained by multiplying Eq. (9) by $R_i n_b^0(R_i)$ on both sides and integrating over the spatial coordinates. Making use of the equilibrium properties of the density distribution in the ground state,

$$\omega_{ib}^2(t) R_i + \frac{g_{bb}}{m_b} \frac{\partial n_b^0(\mathbf{R})}{\partial R_i} + \frac{g_{bf}}{m_b} \frac{\partial n_f^0(\mathbf{R})}{\partial R_i} = 0, \quad (10)$$

after some straightforward algebra one finds,

$$\begin{aligned} \ddot{b}_i(t) + \omega_{ib}^2(t)b_i(t) - \frac{\omega_{ib}^2(0)}{b_i(t) \prod_j b_j(t)} \\ + \frac{g_{bf}}{m_b N_b \langle R_i^2 \rangle_b} \frac{1}{b_i \prod_j b_j} \int d^3 \mathbf{R} \frac{\partial n_f^0(\mathbf{R})}{\partial R_i} R_i n_b^0 \left(\frac{\gamma_i}{b_i} R_i \right) \\ - \frac{g_{bf}}{m_b N_b \langle R_i^2 \rangle_b} \frac{1}{b_i \prod_j b_j} \int d^3 \mathbf{R} \frac{\partial n_f^0(\mathbf{R})}{\partial R_i} R_i n_b^0(\mathbf{R}) = 0, \quad (11) \end{aligned}$$

where $\langle R_i^2 \rangle_b = (1/N_b) \int d^3 \mathbf{R} n_b^0(\mathbf{R}) R_i^2$ is the average size of bosons along the i -axis. The last two terms in Eq. (11), linear in g_{bf} , account for the effects of boson-fermion interaction.

Analogous procedure can also be applied to the fermionic part. We substitute the scaling ansatz Eq. (4) into Boltzmann-Vlasov kinetic equation to get

$$\begin{aligned} \frac{V_i}{\gamma_i^3(t)} \frac{\partial f_0}{\partial R_i} - [\ddot{\gamma}_i(t) + \omega_{if}^2(t)\gamma_i(t)] R_i \frac{\partial f_0}{\partial V_i} \\ - \frac{g_{bf}}{m_b} \frac{1}{\gamma_i(t) \prod_j b_j(t)} \frac{\partial n_b^0(\frac{\gamma_i(t)}{b_i(t)} R_i)}{\partial R_i} \frac{\partial f_0}{\partial V_i} = 0, \quad (12) \end{aligned}$$

where $R_i = r_i/b_i(t)$. Using the equilibrium properties of the distribution function,

$$V_i \frac{\partial f_0}{\partial R_i} - \omega_{if}^2(0) R_i \frac{\partial f_0}{\partial V_i} - \frac{g_{bf}}{m_b} \frac{\partial n_b^0(R_i)}{\partial R_i} \frac{\partial f_0}{\partial V_i} = 0, \quad (13)$$

to replace the first term of Eq. (12) by a linear superposition of $R_i(\partial f_0/\partial V_i)$ and $(\partial n_b^0(R_i)/\partial R_i)(\partial f_0/\partial V_i)$, and taking the moment of $R_i V_i$ (namely, $(1/N_f) \int R_i V_i [Eq.(12)] d^3 \mathbf{R} d^3 \mathbf{V}$), we finally obtain:

$$\begin{aligned} \ddot{\gamma}_i(t) + \omega_{if}^2(t)\gamma_i(t) - \frac{\omega_{if}^2(0)}{\gamma_i^3(t)} \\ + \frac{g_{bf}}{m_f N_f \langle R_i^2 \rangle_f} \frac{1}{\gamma_i \prod_j \gamma_j} \int d^3 \mathbf{R} \frac{\partial n_b^0(\mathbf{R})}{\partial R_i} R_i n_f^0 \left(\frac{b_i}{\gamma_i} R_i \right) \\ - \frac{g_{bf}}{m_f N_f \langle R_i^2 \rangle_f} \frac{1}{\gamma_i^3} \int d^3 \mathbf{R} \frac{\partial n_b^0(\mathbf{R})}{\partial R_i} R_i n_f^0(\mathbf{R}) = 0, \quad (14) \end{aligned}$$

where $\langle R_i^2 \rangle_f = \frac{1}{N_f} \int d^3 \mathbf{R} n_f^0(\mathbf{R}) R_i^2$.

The coupled set of differential equations (11) and (14) is a generalization of Eqs. (5) and (6) in the presence of the boson-fermion coupling. It determines the coupled dynamics of the condensate and degenerate Fermi gas in the collisionless regime as far as the assumption of the simple scaling solution is valid. We shall only be interested in the evolution of $b_i(t)$ and $\gamma_i(t)$ with initial condition of $b_i(0) = 1$, $\gamma_i(0) = 1$, $\dot{b}_i(0) = 0$, and $\dot{\gamma}_i(0) = 0$ ($i = \perp$ or z), in case of switching off the trap suddenly at $t = 0$, *i.e.*, $\omega_{ib,f}(t > 0) = 0$. Our final aim is to calculate the aspect ratio of the condensate and the Fermi gas defined as $\lambda b_\perp(t)/b_z(t)$ and $\lambda \gamma_\perp(t)/\gamma_z(t)$, which are actually measured in experiment. According to Eqs. (11)

and (14), the whole process of our numerical calculations in this paper consists of three stages. First, one has to find the equilibrium ground-state densities: $n_b^0(\rho, z)$ and $n_f^0(\rho, z)$ at very low temperature, which *approximately* satisfy the following coupled equations in the Thomas-Fermi approximation [14],

$$\begin{aligned} V_{ho}^b(\rho, z) + g_{bb} n_b^0(\rho, z) + g_{bf} n_f^0(\rho, z) = \mu_b, \\ \frac{\hbar^2}{2m_f} (6\pi^2 n_f^0(\rho, z))^{2/3} + V_{ho}^f(\rho, z) + g_{bf} n_b^0(\rho, z) = \mu_f, \quad (15) \end{aligned}$$

where $\mu_{b,f}$ is the chemical potential. It is convenient to obtain the solutions of Eq. (15) by iterative insertion of one density distribution in the other equation and numerically searching for μ_b and μ_f yielding the desired number of particles. Then one traces the evolution of $b_i(t)$ and $\gamma_i(t)$ from t to $t + \Delta t$ by evaluating the integrations in Eqs. (11) and (14), which turns out to be the most time-consuming step in the calculations. At the final stage, one computes the radial-to-axial aspect ratio.

III. RESULT AND DISCUSSION

In this work, we have performed numerical simulations with the parameters chosen to reproduce the experimental conditions [3]. The number of bosons and fermions in experiment ($N_b = 2 \times 10^4$ and $N_f = 10^4$) are large enough to ensure the validity of the Thomas-Fermi approximation, *i.e.*, $N_b a_{bb}/a_{ho,\perp}^b \gg 1$ and $N_f \gg 1$ [14,22,23]. We take the harmonic oscillator length $a_{ho,\perp}^b = \sqrt{\hbar/(m_b \omega_{\perp b})}$ and $\hbar \omega_{\perp b}$ as units, and introduce the quantities $\alpha = m_f/m_b$, $\beta = \omega_{\perp f}/\omega_{\perp b}$, and $\lambda = \omega_{zb}/\omega_{\perp b} = \omega_{zf}/\omega_{\perp f}$ to parameterize the different mass of the two components and anisotropy of traps. The constraint $\alpha\beta^2 = 1$ is always satisfied since both bosons and fermions experience the same trapping potential. As in experiment, we have $\alpha = 0.463$, $\beta = 1.47$, and $\lambda = 0.0757$. We have also taken $a_{bb} = +110a_0$ and $a_{bf} = -330a_0$, where $a_0 = 0.529$ Å is the Bohr radius [3]. The most recent measurement suggested a new s -wave scattering length $a_{bf} = -410a_0$ for the mixture of ^{40}K and ^{87}Rb [4,24]. However, the *effective* magnitude of a_{bf} could be indeed lower, considering the possible effect of the gravitational sag [3] and exchange correlations beyond the mean-field approximation [25]. We will return to this point at the end of the paper.

Before presenting the numerical result, it is instructive to briefly analyze the influence of the boson-fermion interaction on the expansion for both species. In the collisionless regime, the effect of the dominated mean-field interaction is two-fold: (*i*) First of all, it influences the profile of the density distribution in the equilibrium ground state. In case of attractive interaction, as shown in Fig. 1, both the density of the condensate and of the degenerate Fermi gas are remarkably enhanced within the central overlap region. The condensate profile narrows

and the central density increases moderately. The effect on the Fermi gas is more pronounced: within the overlap region the fermionic density exhibits a high-density bump on top of the low-density background and the central density is increased by a factor of larger than two [10]. Without considering the mutual attraction during the expansion this enhancement of the density profile, which corresponds to a tighter confinement, will definitely lead to a faster expansion for both species if one turns off the trap potential suddenly. In this paper, we shall consider such kind of fasten-mechanics as a *static effect* of the boson-fermion interaction on the expansion. (ii) On the other hand, the condensate and degenerate Fermi gas also interact with each other during the expansion (especially during the early stages). As a result, with the attractive boson-fermion interaction both species will feel a *running* confinement potential generated by the other species and therefore reduce their expansion rate. This slow-down mechanics is determined by the relative dynamics between the condensate and the degenerate Fermi gas. The smaller the relative expansion velocity is, the more attraction the two species experience. With this respect, it is referred to as a *dynamical effect* of the boson-fermion interaction on the expansion.

Fig. 2 shows the radial-to-axial aspect ratio of the condensate and of the degenerate Fermi gas as a function of the dimensionless expansion time variable τ . Let us firstly concentrate on the condensate. The evolution of the aspect ratio with $a_{bf} = -330a_0$ (the dashed line in Fig. 2a) agrees qualitatively with the experimental result (the solid circles). This agreement is remarkable, considering there is no adjustable parameter in the numerical calculations and the simplicity of our model.

In order to better understand the role of static and dynamical effect of the mean-field boson-fermion interaction on the expansion of the condensate in some details, we expand the density distribution of the Fermi gas around the center by using the fact that in experiment the Fermi gas distributes more widely than the condensate due to the Fermi statistics, and rewrite Eq. (11) into a more physically transparent form,

$$\ddot{b}_i(t) - \frac{\omega_{ib}^2}{b_i(t) \prod_j b_j(t)} + \frac{A\omega_{ib}^2 b_i(t)}{\gamma_i^2(t) \prod_j \gamma_j(t)} - \frac{A\omega_{ib}^2}{b_i(t) \prod_j b_j(t)} \approx 0, \quad (16)$$

where

$$A \approx \frac{g_{bf}}{m_b N_b (R_i^2)_b \omega_{ib}^2} \int d^3 \mathbf{R} \frac{\partial n_f^0(\mathbf{R})}{\partial R_i} R_i n_b^0(\mathbf{R}). \quad (17)$$

Mathematically, the dynamical and static effects are represented by the last two terms in Eq. (16), respectively. Moreover, recalling the free expansion of a pure condensate as shown in Eqs. (5) and (7), the quantity $\omega_{ib}(1+A)^{1/2}$ can in fact be interpreted as an effective trapping frequency experienced by the condensate in ground state. The value of A can further be roughly

extracted from the change of the bosonic density distribution due to the boson-fermion attraction. The estimated value of $A \approx 40\%$ and the corresponding increase of the trapping frequency $\Delta\omega/\omega \approx 20\%$ [26] is two times larger than that used in the fitting in Ref. [3] as we mentioned earlier in the beginning of introduction. This discrepancy can be easily resolved if we consider the dynamical effect of the attraction on the expansion. Indeed, by inserting the scaling solution for elongated traps at first order in λ in Eq. (16), $b_\perp(\tau) = \sqrt{1+(1+\delta)^2\tau^2}$ (δ represents the *net* increase of the trapping frequency), $\gamma_\perp(\tau) \approx \sqrt{1+\beta^2\tau^2}$, $b_z(\tau) \approx 1$, and $\gamma_z(\tau) \approx 1$, one obtains

$$\delta = \beta \left[\frac{(\beta^4 + 4A(1+A))^{1/2} - \beta^2}{2A} \right]^{1/2} - 1. \quad (18)$$

By substituting $\beta = 1.47$ and $A \approx 40\%$ into the above equation, one finds $\delta = 12\%$, in good agreement with the value of 10% used in Ref. [3]. In other words, on the expansion of the ^{87}Rb condensate, the static effect of the mean-field attraction dominates over the dynamical one. If measured in units of increase of the trapping frequency, they contribute around +20% and -8%, respectively.

As explicitly shown in the third term in the left side of the Eq. (16), the dynamical effect of the mean-field attraction on the expansion of the condensate is closely related to the relative dynamics between the condensate and the degenerate Fermi gas, and specifically, related to the value of $\beta = \omega_f/\omega_b$. In Fig. 3 the evolution of the aspect ratio of the condensate and of the degenerate Fermi gas is plotted against the dimensionless expansion time. For both species, the aspect ratio decreases as one lowers the value of β , suggesting that the dynamical effect of the mean-field attraction becomes more and more important with decreasing β . Precisely at $\beta = 1$, where $b_\perp(\tau) = \gamma_\perp(\tau)$, the static and dynamical effects for the condensate are compensated with each other. As a result, the aspect ratio is almost the same as that of a pure condensate. Note that although the above result for $\beta \leq 1$ is not realistic for the mixture of ^{40}K and ^{87}Rb in the LENS experiment, it might be relevant to the system of ^6Li - ^7Li and ^{40}K - ^{41}K , in which $\beta \approx 1$.

The evolution of aspect ratio of the degenerate Fermi gas, on the other hand, is also determined by the competition between the static and dynamical effect of the mean-field attraction. As shown in Figs. 2b and 3b, contrary to the condensate, the dynamical effect for the Fermi gas always dominates and the aspect ratio is less than that of a pure Fermi gas.

We now turn to consider the dependence of the aspect ratio on the strength of boson-fermion interaction. In the first experiments at LENS [3], only the absolute magnitude of a_{bf} , and not its sign, was *directly* determined. It is therefore interesting to study the expansion also in case of repulsive interaction. In Fig. 2 the aspect ratio for $a_{bf} = +330a_0$ (dotted line) is compared

with the result for $a_{bf} = -330a_0$, showing that the behavior of the latter is closer to the experiment points. The fact that boson-fermion interaction is indeed negative has been subsequently confirmed by the observation of the mixture collapse [4]. In order to understand which is the general behavior in passing from negative to positive values of the interspecies scattering length, in Fig. 4 we show the aspect ratio of the condensate and of the degenerate Fermi gas as a function of g_{bf}/g_{bb} at a fixed expansion time. For the condensate, the aspect ratio has a parabolic shape with the minimum located at $g_{bf}/g_{bb} = 0.5$. The possible reason is that in the region of $g_{bf}/g_{bb} < 0$ and $g_{bf}/g_{bb} > 1$, the condensate is always tightly confined by either the attractive or strong repulsive boson-fermion interaction and then the aspect ratio is increased by the dominant static effect of mean-field interaction. In contrast, the aspect ratio of the Fermi gas increases monotonically with increasing the value of g_{bf}/g_{bb} up to $g_{bf}/g_{bb} \approx 2$. It is interesting to note that in principle it is possible to tune g_{bf} by using Feshbach resonances in experiment.

Up to now, we have restricted the discussion to the collisionless regime. In the opposite hydrodynamic regime, the collision terms dominate over the mean-field terms [16]. For the condensate, to ease the analysis we shall still neglect the term Γ_{coll} in the right side of Eq. (1), by assuming that the dynamics of the condensate is less affected by the collisions with the Fermi gas since the condensate always keeps itself in the hydrodynamic regime. For the degenerate Fermi gas, we resort to the Euler equation of motion [17,18], which can be deduced from Boltzmann-Vlasov kinetic equation under the assumption of local equilibrium. The detailed expression of the coupled set of differential equations for $b_i(t)$ and $\gamma_i(t)$ in this regime can be found in Ref. [21]. The predictions of these equations are reported in Fig. 5. The aspect ratio of the condensate is affected by the collisions only in a minor way, which might be understood from the assumption of the vanishing value of Γ_{coll} . For the degenerate Fermi gas, in contrast, the aspect ratio changes remarkably from the collisionless regime to the hydrodynamic one. This is consistent with the result in Ref. [13], where the *same* Euler equation of motion has been used to describe the expansion of a *superfluid* Fermi gas [27]. Note that the expansion of a strongly interacting degenerate Fermi gas has been recently demonstrated in Ref. [28], and has been explained qualitatively by the theory of Menotti *et al.* [13]. However, a stringent test of distinguishing the system from the normal hydrodynamic phase to the superfluid phase is lacking in the experiment [29].

IV. SUMMARY

In conclusion, we have studied the effect of the boson-fermion interaction on the expansion of a boson-fermion

mixture, within a simple scaling ansatz. We have considered in some details the interplay of the so-called static and dynamic effect of the mean-field interaction on the expansion. The former is caused by the modified density profiles in the equilibrium ground state, while the latter refers to the interaction between the condensate and Fermi gas during the first stage of the expansion. These two effects are compensated with each other. Which one plays the most important role depends on the detailed parameters of the system.

For the mixture of ^{40}K and ^{87}Rb , the static effect is dominant for the expansion of the condensate and its aspect ratio is inverted more rapidly than that of a pure condensate. This feature has been observed in the experiment, and also well reproduced by our numerical simulations. For the degenerate Fermi gas, on the other hand, the dynamical effect becomes important. As a result, its aspect ratio is less than that of a pure Fermi gas. This prediction needs further experimental investigation.

At the end of this paper, several remarks are in order: (i) The above results are based on the assumption of the simple scaling solution. The justification of using such scaling ansatz on the problem of collective excitations has been discussed in Ref [21] by the authors. We have shown that this approximation is equivalent to the sum-rule approach. However, on the problem of the expansion, its validity deserves a further study (especially for the degenerate Fermi gas), though our numerical results for the condensate are in reasonable agreement with the experiment. (ii) In a recent preprint, the importance of the corrections due to exchange-correlation energy on the ground state of mixture ^{40}K and ^{87}Rb has been discussed [25]. Such corrections on the expansion can also be investigated by adding the exchange correlations in the local density approximation. (iii) For the mixture of ^{40}K and ^{87}Rb , the recent measurements give a more accurate value of the *s*-wave interspecies scattering length: $a_{bf} = -410a_0$ [4,24]. In Fig. 6, we show the aspect ratio for such large negative scattering length without considering the effect of different gravitational sag for ^{40}K and ^{87}Rb . The result with inclusion of the exchange-correlation term is also plotted by the dotted line. For the condensate the calculated aspect ratio is larger than the experimental result. This discrepancy is *partly* due to the possible effect of the gravitational sag [27]. (iv) Finally, a careful consideration of the role of collisions is needed.

V. ACKNOWLEDGMENTS

We acknowledge stimulating discussions with G. Modugno. One of us (X.-J. Liu) wishes to thank the Abdus Salam International Centre for Theoretical Physics (ICTP) for their hospitality during the early stages of this work. X.-J. Liu is supported by the CAS K.C.Wang Post-doctoral Research Award Fund, the Chinese Post-

-
- [1] A. G. Truscott, K. E. Strecker, W. I. McAlexander, G. B. Partridge, and R. G. Hulet, *Science* **291**, 2570 (2001); F. Schreck, L. Khaykovich, K. L. Corwin, G. Ferrari, T. Bourdel, J. Cubizolles, and C. Salomon, *Phys. Rev. Lett.* **87**, 080403 (2001).
- [2] Z. Hadzibabic, C. A. Stan, K. Dieckmann, S. Gupta, M. W. Zwierlein, A. Gorlitz, and W. Ketterle, *Phys. Rev. Lett.* **88**, 160401 (2002).
- [3] G. Roati, F. Riboli, G. Modugno, and M. Inguscio, *Phys. Rev. Lett.* **89**, 150403 (2002).
- [4] G. Modugno, G. Roati, F. Riboli, F. Ferlaino, R. J. Brecha, and M. Inguscio, *Science* **297**, 2240 (2002).
- [5] H. Heiselberg, C. J. Pethick, H. Smith, and L. Viverit, *Phys. Rev. Lett.* **85**, 2418 (2000).
- [6] M. J. Bijlsma, B. A. Heringa, and H. T. C. Stoof, *Phys. Rev. A* **61**, 053601 (2000).
- [7] D. O. Edwards, D. F. Brewer, P. Seligman, M. Skertic, and M. Yaquib, *Phys. Rev. Lett.* **15**, 773 (1965).
- [8] A. C. Anderson, D. O. Edwards, W. R. Roach, R. E. Sarwinski, and J. C. Wheatley, *Phys. Rev. Lett.* **17**, 367 (1966).
- [9] R. Roth and H. Feldmeier, *Phys. Rev. A* **65**, 021603(R) (2002).
- [10] R. Roth, *Phys. Rev. A* **66**, 013614 (2002).
- [11] S. Stringari, *Phys. Rev. Lett.* **77**, 2360 (1996).
- [12] D. Guéry-Odelin, *Phys. Rev. A* **66**, 033613 (2002).
- [13] C. Menotti, P. Pedri and S. Stringari, *Phys. Rev. Lett.* **89**, 250402 (2002).
- [14] K. Mølmer, *Phys. Rev. Lett.* **80**, 1804 (1998).
- [15] At low temperature, the main contribution to the collision term comes from the collisions between a fermion and a condensed atom, in which the fermion is scattered into another state, while the condensed boson becomes a thermal atom. In the Hartree-Fock approximation, one may derive the expressions for the dissipation terms as: $-\Gamma_{coll} = -\frac{n_c g_{bf}^2}{(2\pi)^5 \hbar^7} \int d\mathbf{q} d\mathbf{p}_1 d\mathbf{p}_2 \delta_\epsilon \delta_{\mathbf{p}} \times \left[(1 + \tilde{f}(\mathbf{q}))(1 - f(\mathbf{p}_2))f(\mathbf{p}_1) - \tilde{f}(\mathbf{q})(1 - f(\mathbf{p}_1))f(\mathbf{p}_2) \right]$ and $I_{coll} = \frac{n_c g_{bf}^2}{(2\pi)^2 \hbar^4} \int d\mathbf{q} d\mathbf{p}_1 d\mathbf{p}_2 \delta_\epsilon \delta_{\mathbf{p}} (\delta(\mathbf{p} - \mathbf{p}_2) - \delta(\mathbf{p} - \mathbf{p}_1)) \times \left[(1 + \tilde{f}(\mathbf{q}))(1 - f(\mathbf{p}_2))f(\mathbf{p}_1) - \tilde{f}(\mathbf{q})(1 - f(\mathbf{p}_1))f(\mathbf{p}_2) \right]$, where δ_ϵ and $\delta_{\mathbf{p}}$ are the usual delta functions accounting for the conservation of momentum and energy. \tilde{f} and f are the single-particle phase-space distribution function for thermal bosons and for fermions, respectively.
- [16] Here, the meaning of “hydrodynamic” refers only to the Fermi gas. For the condensate, it is always in the hydrodynamic regime as described by the Stringari’s hydrodynamic equation.
- [17] M. Amoruso, A. Minguzzi, S. Stringari, M. P. Tosi, and L. Vichi, *Eur. Phys. J. D* **4**, 261(1998).
- [18] Yu. Kagan, E. L. Surkov, and G. V. Shlyapnikov, *Phys. Rev. A* **55**, R18 (1997).
- [19] Y. Castin and R. Dum, *Phys. Rev. Lett.* **77**, 5315 (1996).
- [20] G. M. Bruun and C. W. Clark, *Phys. Rev. A* **61**, 061601 (2000).
- [21] X.-J. Liu and H. Hu, cond-mat/0212169 (2002), to appear in *Phys. Rev. A*.
- [22] N. Nygaard and K. Mølmer, *Phys. Rev. A* **59**, 2974 (1999).
- [23] D. A. Butts and D. S. Rokhsar, *Phys. Rev. A* **55**, 4346 (1997).
- [24] F. Ferlaino, R. J. Brecha, P. Hannaford, F. Riboli, G. Roati, G. Modugno, and M. Inguscio, cond-mat/0211051 (2002).
- [25] A. P. Albus, F. Illuminati, and M. Wilkens, cond-mat/0211060 (2002).
- [26] We have used two methods to extract the value of $\Delta\omega/\omega$. One is to use the relation $n_b(0) \propto \omega^{6/5}$, and the other is $(\langle x^2 + y^2 \rangle)^{1/2} \propto \omega^{-2/5}$. Both of them are valid for the parabolic confinement for a pure condensate. From Fig. 1a, the former relation gives $\Delta\omega/\omega = 25\%$, and the latter gives $\Delta\omega/\omega = 17\%$. The possible reason for the discrepancy might be due to the fact that the density profile of the condensate in mixture is not perfectly parabolic. Nevertheless, a rough estimate of $\Delta\omega/\omega \approx 20\%$ is convincing.
- [27] If the critical temperature for superfluidity is high enough, both the normal the superfluid phases may be governed by the *same* hydrodynamic regime over the whole range of relevant temperatures.
- [28] K. M. O’Hara, S. L. Hemmer, M. E. Gehm, S. R. Granade, and J. E. Thomas, *Science* **298**, 2179 (2002).
- [29] L. Pitaevskii and S. Stringari, *Science* **298**, 2144 (2002).
- [30] Since it is hard to study the possible effect of the gravitational sag on the expansion, we have considered the effect of gravitational sag on the equilibrium density profile in the ground state without the inclusion of exchange correlations, by solving the 3D Gross-Pitaevskii equation for the condensate and using Thomas-Fermi approximation for the degenerate Fermi gas. Our result shows that it only plays a *minor* role compared with changing a_{bf} from $-410a_0$ to $-330a_0$. Therefore, the inclusion of the possible effect of gravitational sag may not be able to fully resolve the discrepancy mentioned in the paper.

Figures Captions

FIG. 1. The equilibrium density distribution of the condensate (a) and of the degenerate Fermi gas (b) along the radial direction for two different values of a_{bf} : $a_{bf} = 0$ (full line) and $a_{bf} = -330a_0$ (dashed line), where $a_0 = 0.529 \text{ \AA}$ is the Bohr radius. We have taken $a_{bb} = 110a_0 = 5.82 \text{ nm}$. The coordinate ρ and the density $n_{b,f}$ are measured in units of the harmonic oscillator length $a_{ho,\perp}^b$ and $(a_{ho,\perp}^b)^3$, respectively.

FIG. 2. The radial-to-axial aspect ratio of the condensate (a) and of the degenerate Fermi gas (b) as a function of the dimensionless expansion time variable τ with a boson-fermion s -wave scattering length $a_{bf} = 0$ (solid line), $-330a_0$ (dashed line), and $+330a_0$ (dotted line). For comparison, the experimental data (solid circles) are also plotted. One unit of τ corresponds to 0.738 ms in the experiment [3]. Note that the aspect ratio for the condensate with $a_{bf} = -330a_0$ agrees qualitatively with the experiment, without any adjustable parameters. Note also that in the experiment, the typical absorption image is taken at $\tau = 21$ (or $t = 15.5$ ms) for the condensate and at $\tau = 6.1$ (or $t = 4.5$ ms) for the degenerate Fermi gas.

FIG. 3. Aspect ratio of the condensate (a) and of the degenerate Fermi gas (b) at $a_{bf} = -220a_0$ for various values of $\beta = \omega_{\perp f}/\omega_{\perp b}$. The aspect ratio for $\beta = 1.0$ in figure (a) is almost the same as that of a pure BEC. Note that the value of $a_{bf} = -220a_0$ is not realistic in experiment. However, if we take $a_{bf} = -330a_0$, we cannot find out the density distributions of the equilibrium ground state for $\beta = 1.0$ or $\beta = 0.85$ within Thomas-Fermi approximation. The possible reason is that the mixture composed of $N_b = 2 \times 10^4$ and $N_f = 10^4$ will collapse when $\beta \leq 1$.

FIG. 4. (a) The aspect ratio of the condensate at $\tau = 21$ as a function of g_{bf}/g_{bb} . (b) The aspect ratio of the Fermi gas at $\tau = 6.1$ as a function of g_{bf}/g_{bb} . In principle, it is possible to tune g_{bf} by using Feshbach resonances. Note that $g_{bf}/g_{bb} = 1.5875a_{bf}/a_{bb}$ for the mixture of ^{40}K and ^{87}Rb . In the experiment, $a_{bf} = -330a_0$ corresponds to $g_{bf}/g_{bb} = -4.7625$.

FIG. 5. Comparison of the aspect ratio of the condensate (a) and of the degenerate Fermi gas (b) at $a_{bf} = -330a_0$ in the collisionless and hydrodynamic regime. For comparison, the result for the decoupled boson-fermion mixture in the collisionless regime are also plotted by the solid lines.

FIG. 6. Aspect ratio of the condensate (a) and of the degenerate Fermi gas (b) at $a_{bf} = -410a_0$ with and without the inclusion of the exchange correlation term.

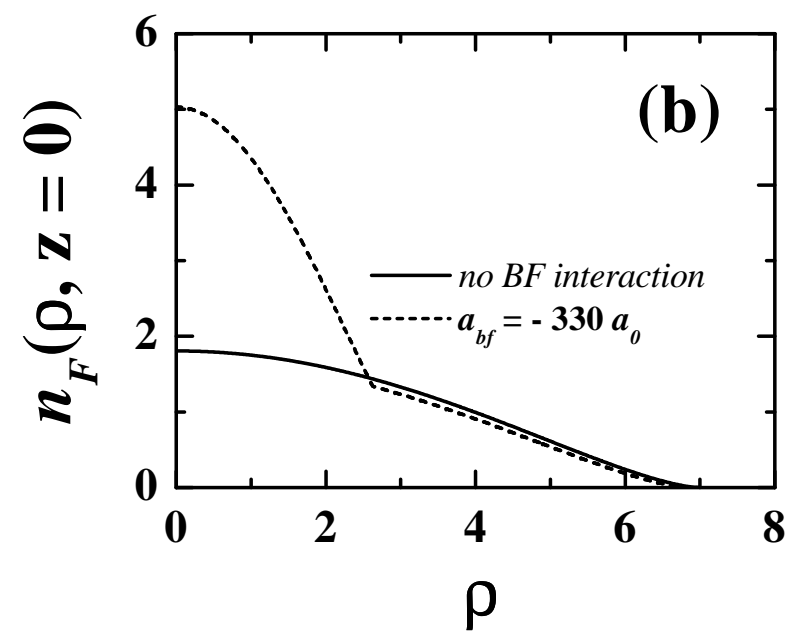
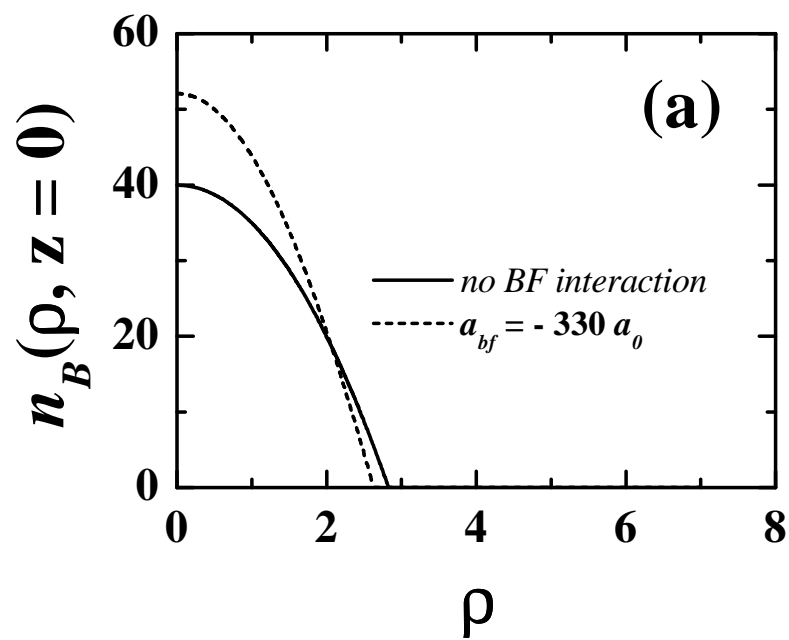


Figure 1, Expansion of a quantum degenerate boson-fermion mixture

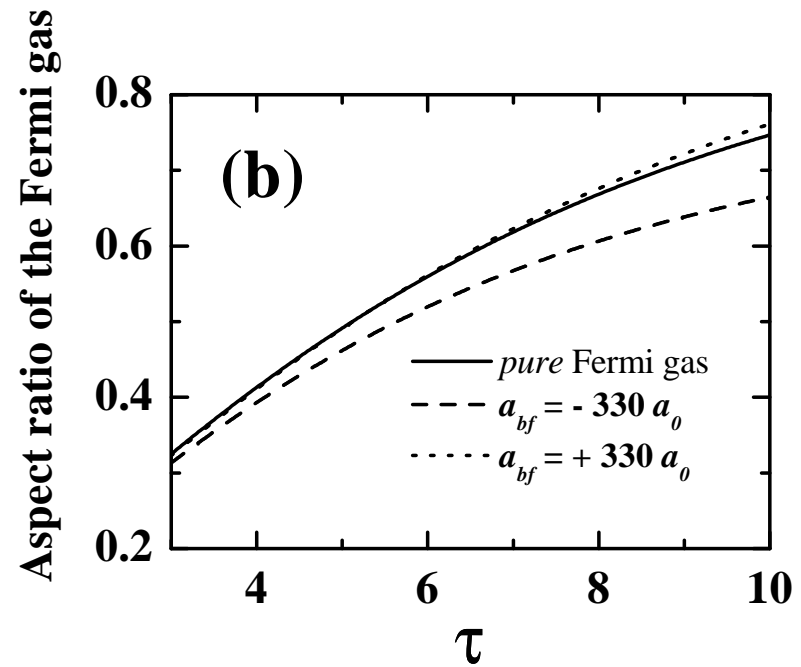
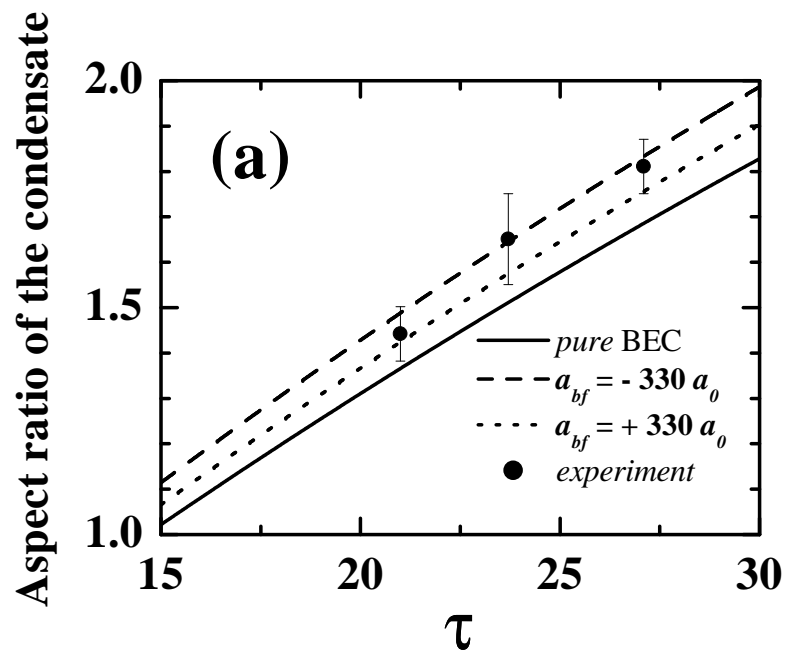


Figure 2, Expansion of a quantum degenerate boson-fermion mixture

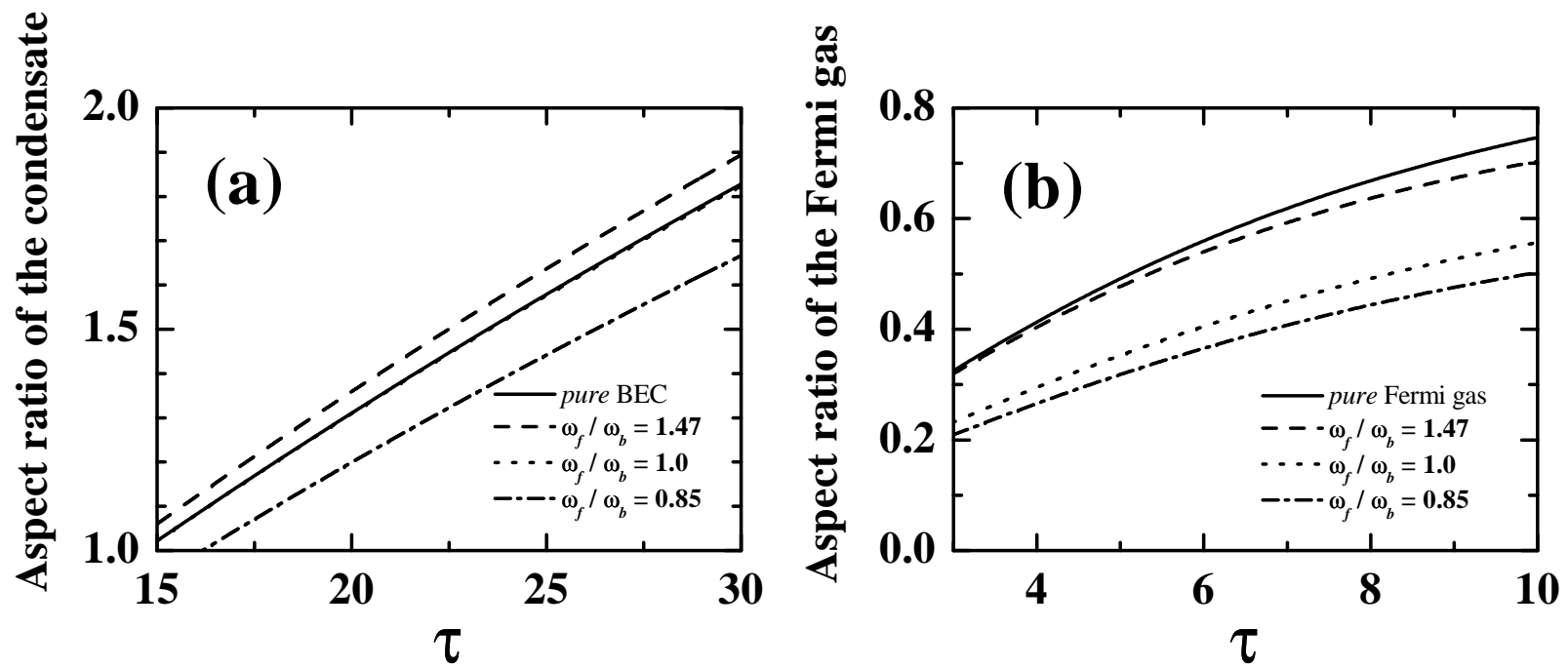


Figure 3, Expansion of a quantum degenerate boson-fermion mixture

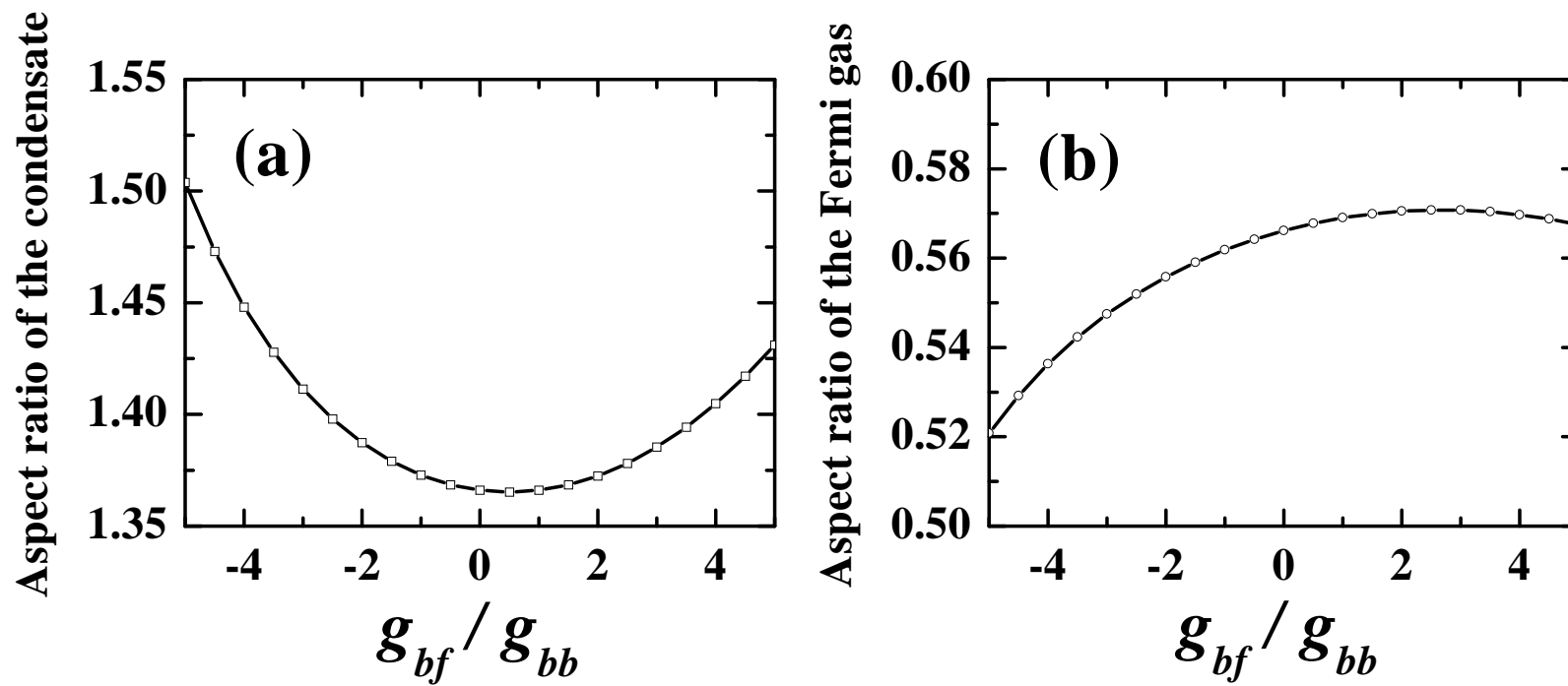


Figure 4, Expansion of a quantum degenerate boson-fermion mixture

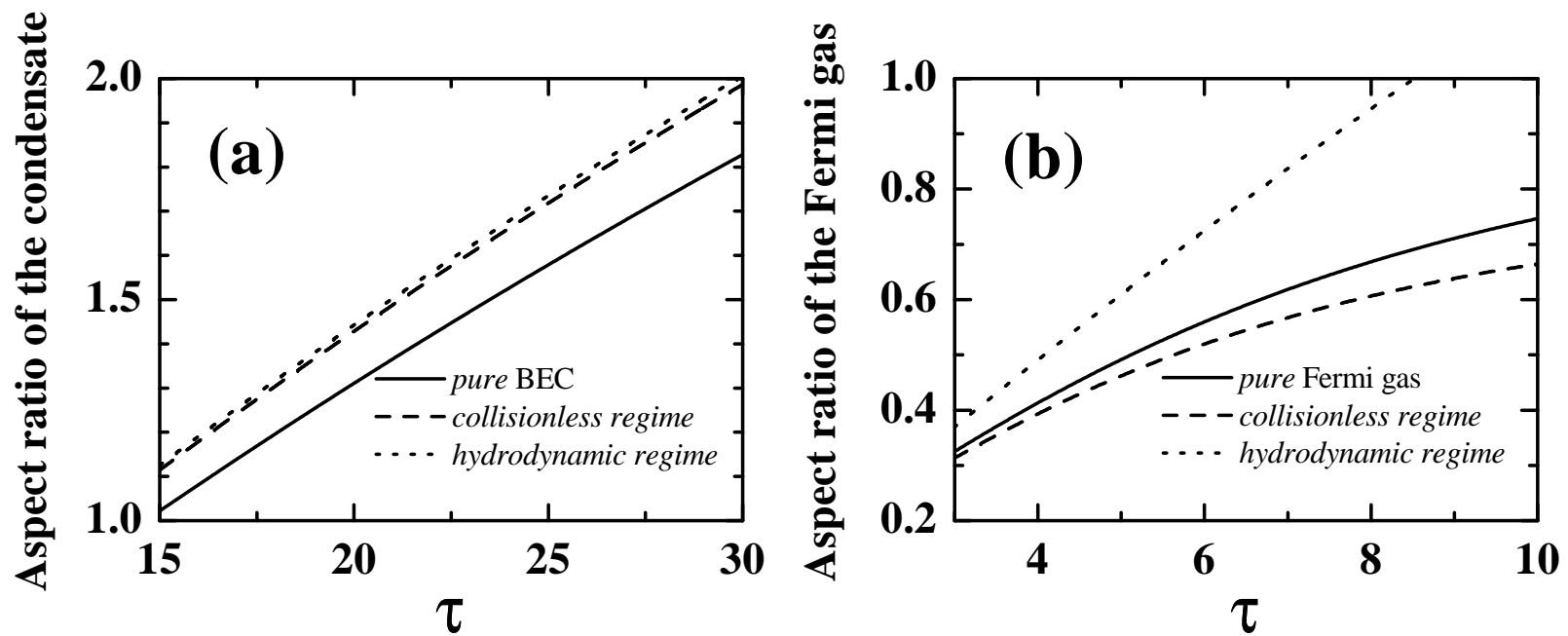


Figure 5, Expansion of a quantum degenerate boson-fermion mixture

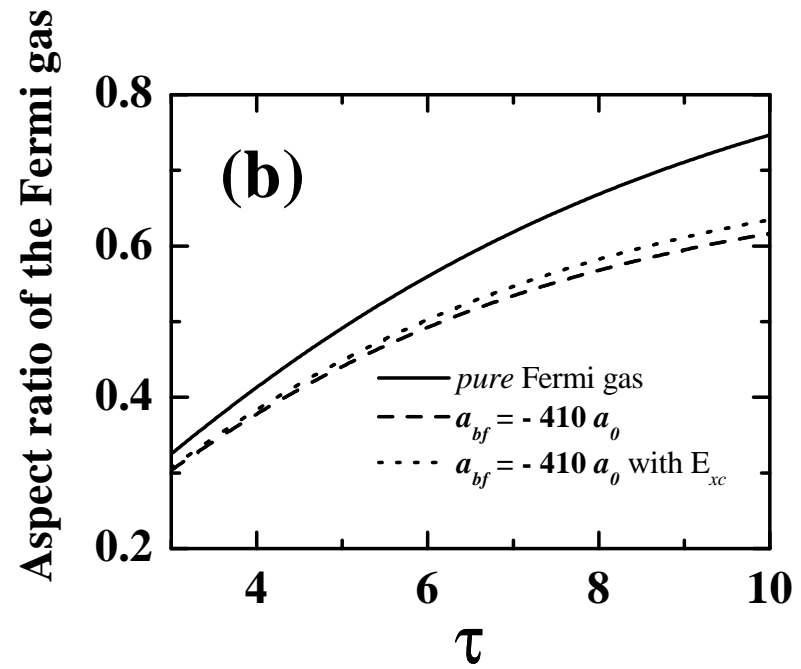
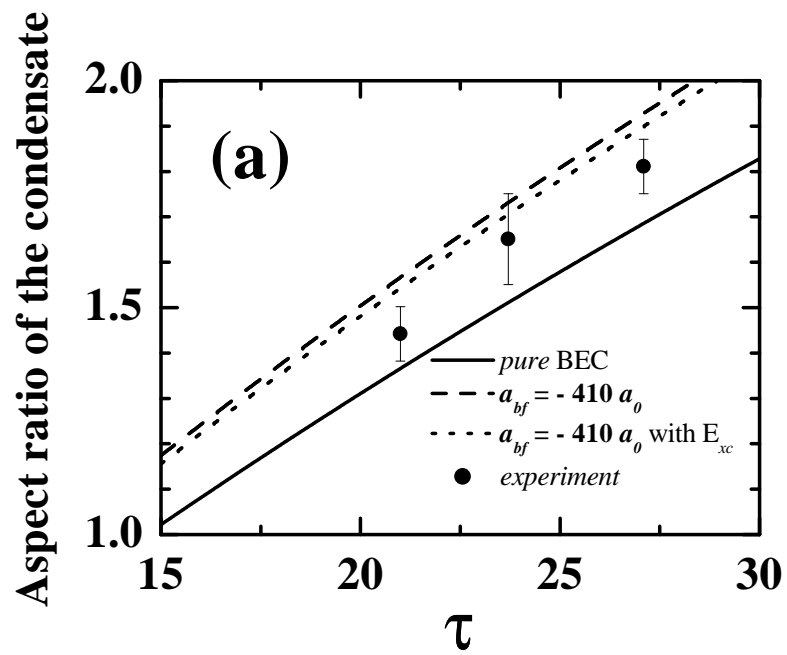


Figure 6, Expansion of a quantum degenerate boson-fermion mixture